Asian Journal of Chemistry; Vol. 31, No. 4 (2019), 813-819

ASIAN JOURNAL OF CHEMISTRY

https://doi.org/10.14233/ajchem.2019.21745

# Synthesis, Characterization, Photocatalytic Activities and Reusability of Eu-ZnO-Ag Nanoparticles using Sunlight/LEDs Illuminations

Y. JERLIN JOSE[1], S. JOSEPH SELVARAJ[1] and M. MANJUNATHAN[2,*]

[1]Department of Chemistry St. Joseph's College, Tiruchirappalli-620002, India
[2]Department of Chemistry, BWDA Arts and Science College, Villupuram-604304, India

*Corresponding author: E-mail: manjunath876@gmail.com

*Received*: 6 October 2018; *Accepted*: 7 January 2019; *Published online*: 27 February 2019; AJC-19290

Photocatalyst (Eu–ZnO–Ag) was synthesized by precipitation-decomposition process. The characterization catalyst by phase and size of catalyst by powder-XRD, morphology of catalyst by FE-SEM and optical properties by UV-visible and emission spectroscopy. The photocatalytic action of Eu–ZnO–Ag was investigated in the photodegradation of methylene blue dye in water under LEDs/solar light. Eu–ZnO–Ag catalyst is indicating the excellent activity than Ag–ZnO, Eu–ZnO commercial ZnO/$TiO_2$ nanoparticles. Co-dopants (Eu/Ag) shift the light absorbance of ZnO toward visible region. Factor affecting of photodegrdation study by dose, dye, solution pH on of methylene blue dye present solar/LEDs. The Eu–ZnO–Ag is established to be reusable photocatalyst. A potential photodegradation of methylene blue mechanism was discussed under illuminations LEDs/solar light.

**Keywords: Nanoparticles, Sunlight, LEDs, Photodegradation of methylene blue dye.**

## INTRODUCTION

Photocatalysis is shown excellent activity for solving many current issues, Industries waste water such as textiles, pharmaceuticals, plastics, rubber, printing, *etc.*, May transport great terrorization to the water environment, due to the waste water pollutants and harmful chemicals affected the environmental area and liveliness issues. These types of pollutants are challenge and useful research in the environmental science. Semiconductor and metal doped-semiconductor recommend the potential for exclusion of toxic chemicals through their adsorption and photochemical methods are wide applicability [1-3]. Heterogeneous photo-catalysis with metal doped-metal-oxides are widely investigation of degradation of air and waste water, but also for alternative energy materials. Photocatalysts of pure/doped $TiO_2$, ZnO and metal doped metal-oxides are applied to a diversity of environmental processes such as remediation of harmful chemicals and water pollutants [4-8].

The depend of metals, such as Cu [9], Ag [10] and Au [11] on semiconductor oxides are reported to increase their catalytic activity Recently, concurrent doping of two kinds of ions into metal-oxides materials has involved considerable interest, as it could result in a higher photocatalytic activity and performance compared with mono metal ion doping into semiconductors, such as $Ag^+$ and lanthanide-doped ZnO [12] observed good performance for its exclusive 4*f* electron configuration of lanthanides. Eu-doped ZnO have attracted interest due to the $Eu^{3+}/Eu^{2+}$ redox couple [13,14] Many studies have shown that La doping enhances the photocatalytic activity of ZnO/$TiO_2$ [15-17]. The reported synthesized Sm-ZnO-Ag through precipitation decomposition method, which showed highly excellent photocatalytic activity in thiazin type (methylene blue) degradation [18]. The catalytic performances of the Eu-ZnO-Ag catalysts were investigated in water, catalytic activation for methylene blue degradation, outstandingly performance of Eu-ZnO-Ag was found to have excellent activity and excellent stability in co-catalytic activation of europium/silver for methylene blue dye degradation present of LEDs/solar light illuminations.

## EXPERIMENTAL

The methylene blue dye (99 %) and $Zn(NO_3)_2{\cdot}6H_2O$ (AR), $AgNO_3$ and $Eu(NO_3)_3{\cdot}6H_2O$ were purchased from Sigma-Aldrich and Merck. All the chemical reagents purchased and

used for AR grade without further purifications. All the experiment using triple distilled water is taken to prepare (alkaline $KMnO_4$) experimental solutions. The maintained pH of solution by addition of acid or base before doing irradiation experiment.

**Preparation of Eu–ZnO–Ag nanoparticles:** A precipitation decomposition method is applied to prepare Eu–ZnO–Ag catalyst (**Scheme-I**). A 100 mL of zinc nitrate hexahydrate (0.8 M) and 100 mL of oxalic acid (1.2 M) in triple distilled water used to homogenous was boiled separately. Both are 5 mL of $AgNO_3$ (2 % Ag) solution and 5 mL of $Eu(NO_3)_3$ (8 % Eu) solution added slowly one by one with constant stirring of zinc nitrate bulk solution were heated for 1 h at 60–70 °C. Further adding of oxalic acid into bulk solution. The mixture of $[Eu(NO_3)_3 + AgNO_3 + Zn(NO_3)_2]$ oxalic acid solution was formed. Finally precipitation of Eu-zinc-Ag oxalate occurred when the solution was cooled to room temperature. The Eu-zinc-Ag oxalate powder washed with triple distilled water and dried at 100 °C for 6 h. The Eu-Zinc-Ag oxalate powers were calcinated at 10 °C per mints in a muffle furnace reach the decomposition (450 °C) temperature. The Eu–ZnO–Ag catalyst was collected and used for further analysis. This catalyst contained 8 wt % of Eu. Other catalyst are prepared by same procedure with or without (Ag/Eu) and percentage of metal ions with appropriate amounts of the respective precursors.

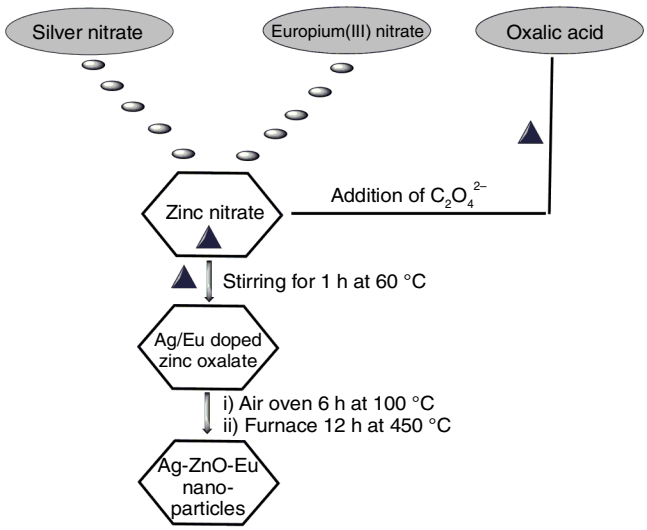


**Scheme-I:** Schematic preparation of Eu–ZnO-Ag nanoparticles

**Analytical methods:** X-ray diffraction pattern was obtained using an X'Pert PRO diffractometer outfitted with Cu-$K_\alpha$ ($\lambda$ = 1.5406 Å) radiation at 2.2 kW (max), The morphology of the catalyst analysis by JEOL JSM-6701F scanning electron microscope. Before SEM measurements, equipped with OXFORD, energy dispersive X-ray microanalysis (EDS). The FT-IR spectra of the nano particles were recorded on a Thermo Nicollet-6700, FT-IR instrument in the range 4000–400 $cm^{-1}$ (KBr pellet technique). A photo illumination was recorded with a Horiba-JobinYvon, SPEX-SF13-11 spectroflourimeter. Optical spectra are recorded in Shimadzu, (UV 2450) double-beam spectrophotometer.

**Photodegradation experiments:** A photochemical reactor designed 50 mL capacity with irradiated with LEDs and solar light illuminations. The Eu-ZnO-Ag was magnetically stirred in absence of light illuminations for 30 min to reach adsorption-desorption equilibrium between the methylene blue dye and photo-catalyst nanoparticles. At expected time intervals, 3 mL of the photodegrdation study of decomposed sample was taken out and centrifuged solution to take away the catalyst for further analysis. The similar condition was followed for Solar light degradation of methylene blue dye, the Solar light illuminations intensity almost constant through the experiments day time 11 AM-3 PM (Tamilnadu state, India) [18].

## RESULTS AND DISCUSSION

### Characterization of catalyst

**Powder XRD analysis:** The XRD patterns of the pure ZnO and Ag-ZnO and Eu–ZnO-Ag nanoparticles., diffraction peaks are found at 31.68 (100), 34.36 (002), 36.18 (101) and 56.56 (110) correspond to wurtzite ZnO planes structure and so reveals that bare ZnO has the wurtzite structure. Fig. 1 shows the XRD pattern of Ag-ZnO and Eu–Ag–ZnO nanoparticles, in addition to the bare ZnO peaks there is a no new peak obtained and intensity decrease when influence of depends (Ag/Eu), so confirms the load the low concentration of Ag/Eu ions this could not be detected by XRD [18,19]. The crystalline sizes of pure/doped ZnO nanoparticles and Eu–Ag–ZnO nanoparticles were determined *via* the Debye–Scherrer equation and are found to be 50 and 36 nm, respectively. The average crystalline size of Eu–Ag–ZnO nanoparticles is lower than of pure ZnO.

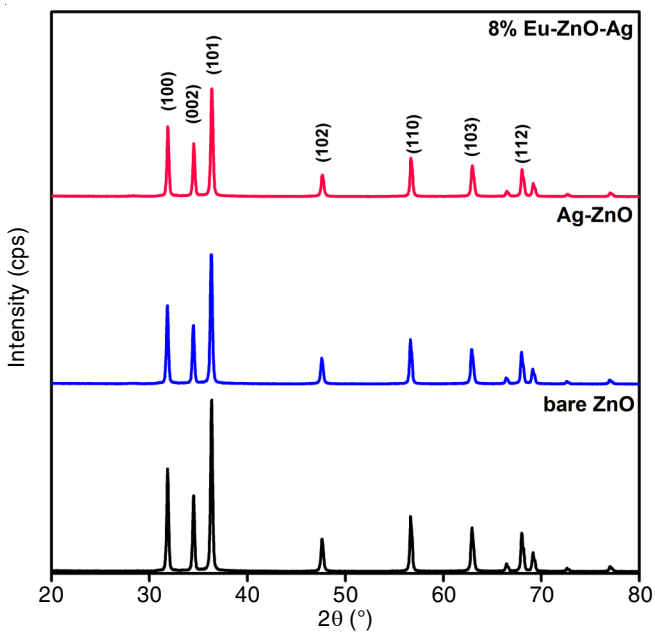


Fig. 1. XRD patterns of ZnO, Ag-ZnO and Eu–ZnO-Ag nanoparticles

**SEM analysis:** The surface and shape of the photocatalyst are considerable parameters as they influence the catalytic activity. The shape and surface of Eu–Ag–ZnO has been analyzed by SEM images. The SEM analysis images (Fig. 2) at different magnifications on different locations are Eu–Ag–ZnO exhibits "hexagonal and chain like" structure of ZnO is clearly indicate wurtzite structure of Eu–Ag–ZnO nanoparticles. The

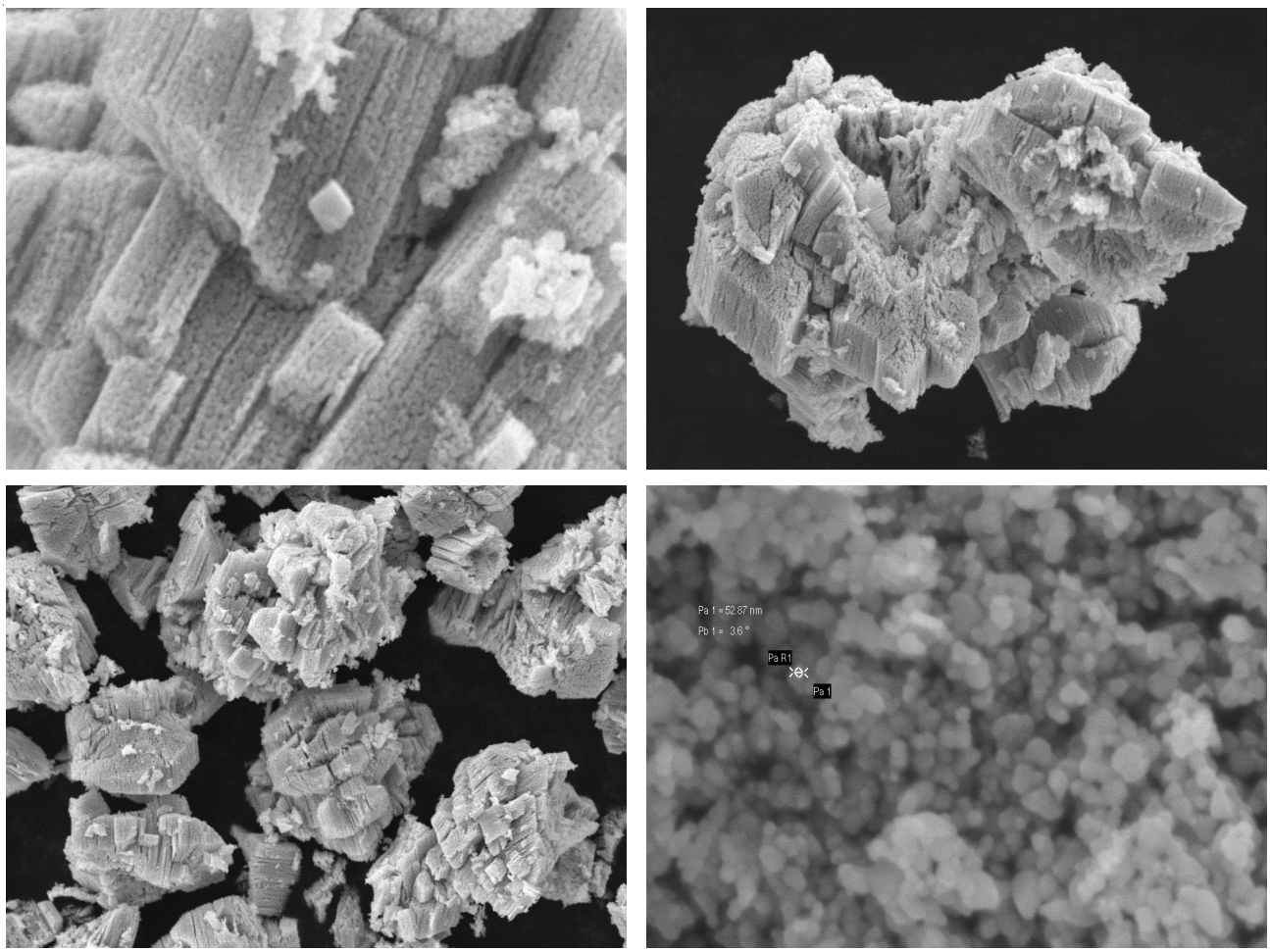

Fig. 2. FE-SEM images at different magnification (1 µm, 2 µm, 200 nm) of 8 % Eu–ZnO–Ag nanoparticles

Eu particles are highly spread over the surface of photocatalyst, similar morphology also observed in 2 % and 4 % Eu–ZnO–Ag catalyst The EDS of Eu–ZnO–Ag reveals the presence of (Fig. 3) Eu, Ag, Zn and O. The particle sizes of catalyst are in the range of 35–200 nm.

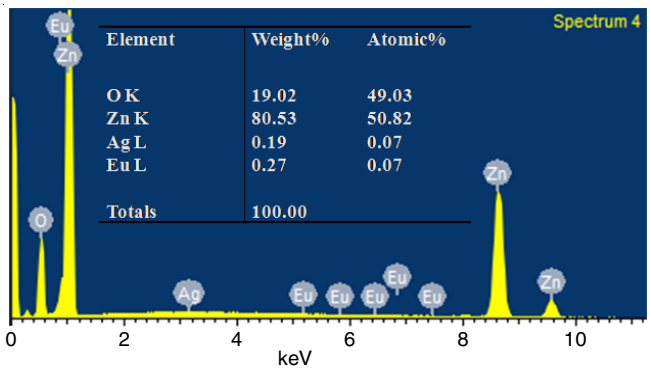


Fig. 3. EDAX images at 8 % Eu–ZnO-Ag nanoparticles

**Optical properties of catalyst:** A red shift absorbed edge from 360 to 420 nm appeared for silver and europium doped in ZnO nanoparticles (Figs. 4 and 5). The red shift in the absorption explains for band gap decreased compare pure ZnO nanoparticles [20] conformed that presence of Eu–ZnO-Ag bonds. It is commonly consider that the red shift is conforming by the new energy level in the band gap (3.01 eV).

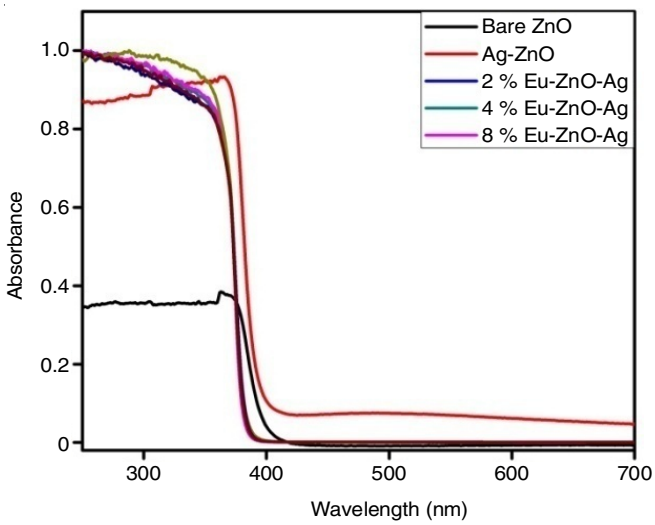


Fig. 4. UV-visible spectra of ZnO, Ag–ZnO and Eu–ZnO–Ag nanoparticles

As a result, Eu–ZnO-Ag has an electron trapping level, which decreases than pure ZnO nanoparticles and the europium doping enhances the visible light absorption capacity of the doped ZnO photocatalyst. The DRS spectra of the obtained and the red shift evidently shows that the sharp band gap produced from Eu ion 4*f* level to ZnO valence or conduction band there is CT spectra [21]. FTIR spectra explain various functional groups and metal-oxide (MO) bond are analyzed.

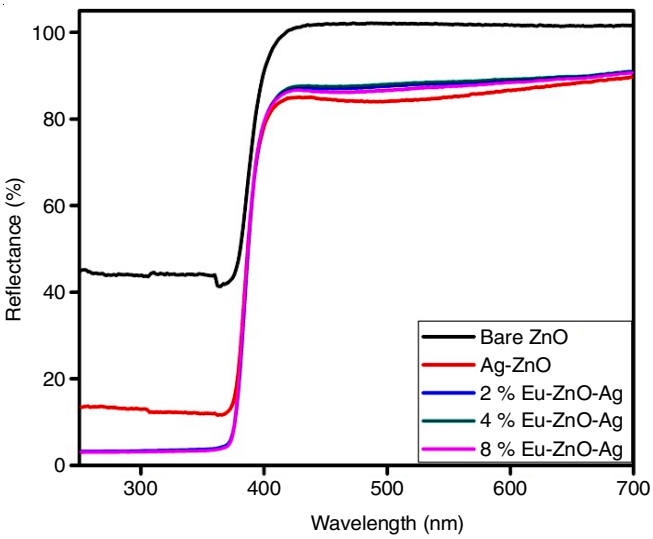


Fig. 5. Diffuse reflectance spectra of ZnO, Ag–ZnO and Eu–ZnO–Ag nanoparticles

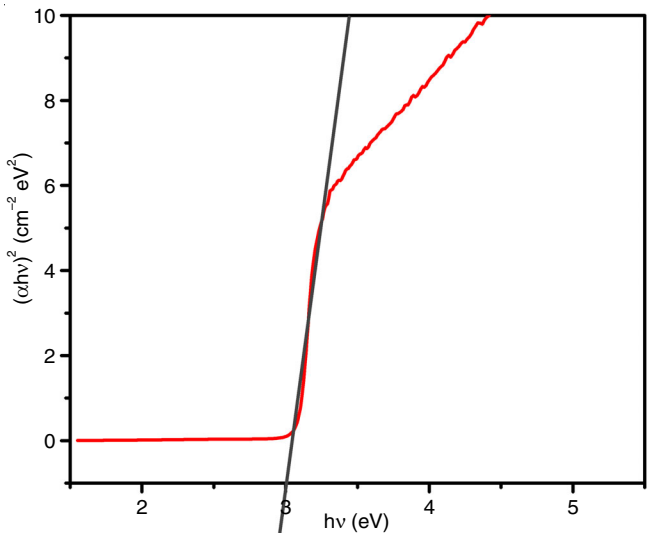


Fig. 7. Plot for (BG) Kubelka-munk function *versus* energy of the light absorbed of catalyst

In the FTIR spectrum, a important band at about 475 and 425 $cm^{-1}$ is assigned to the characteristic stretching/bending mode of Ag-O, Eu-O and Zn-O bond. Absorption band at 3425-3325 $cm^{-1}$ arises due to the stretching mode of O-H group, which reveals the existence of aqueous absorbed by the pure ZnO and doped ZnO nanoparticles (Fig. 6).

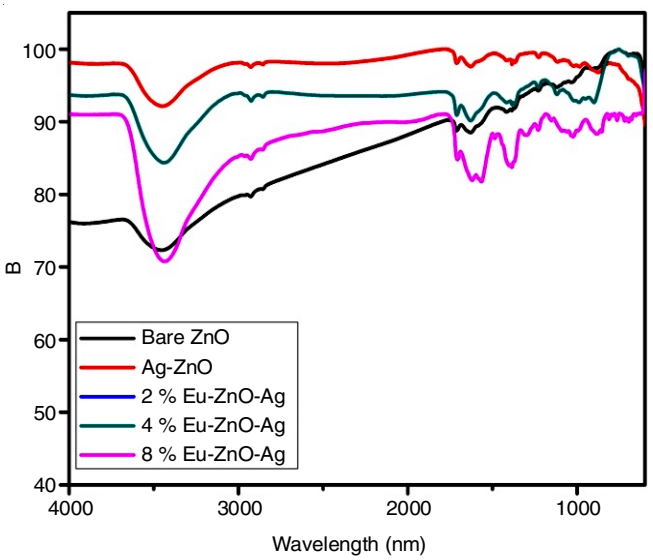


Fig. 6. FT-IR Spectra of ZnO, Ag–ZnO and Eu–ZnO–Ag nanoparticles

Fig. 7 showed the band gap energies by the plot of the modified Kubelka–Munk function, $[F(R)E]^{1/2}$ *vs*. the energy of the absorbed light, we observed the band gap of Eu–ZnO-Ag is 3.01 eV. The pure ZnO nanoparticles showed three emissions bands at 420, 480 and 540 nm (Fig. 8). The doping of Eu/Ag with ZnO do not shift any emission of ZnO but the intensity of emission reduced than pure ZnO nanoparticles (Fig. 5). This photoluminescence intensity changes due to recombination of electron–hole pairs by dopants ions. This reduces the photoluminescence intensity as a result of the reduction of the rate of electron–hole recombination excellent the electron transfer reactions in dye degradation study [18].

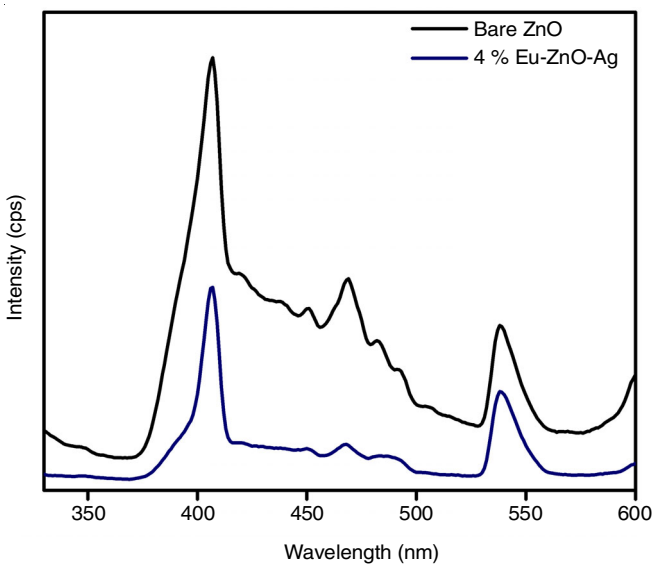


Fig. 8. Photoluminescence spectra of ZnO and 8 % Eu–ZnO-Ag nanoparticles

## Effects of photocatalytic parameters

**Effect of solution pH:** The photodegradation mainly focused on adsorption of the dye molecules on the surface of the photocatalyst. The catalyst adsorption of the methylene blue molecules on pH of the solution depended. The pseudo-first order rate constants for Eu–ZnO-Ag at pH/rate constant are (3) 0.0269, (5) 0.0422, (7) 0.0552, (9) 0.0738 and (11) 0.0482 $min^{-1}$, respectively after the photo catalyst of adsorption equilibrium (30 min) in Fig. 9. It is observed that linearly increase (3-9) in pH from 9 increases the removal efficiency of methylene blue and then decreases. An acidic medium poorer result is obtained due to the suspension of photo-catalyst. The efficient of degradation observed basic medium with (pH–9) adsorption of methylene blue molecules on the surface of the catalyst.

**Effect of catalyst dosage:** Fig. 10 showed photo-degradation pseudo-first order rate constant of methylene blue dye under LEDs light with different catalyst dose amount 1 g (0.0637), 2 g (0.0738), 3 g (0.0729), 4 g (0.0729) and 5 g (0.0728

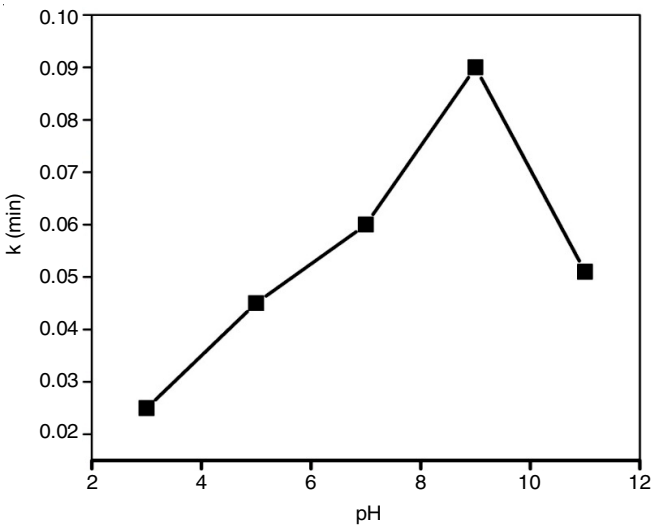


Fig. 9. Effect of solute ion pH; [methylene blue] = $10^{-5}$ $mL^{-1}$, 8 wt % Eu–ZnO–Ag nanoparticles catalysis suspended = 500 mg $L^{-1}$, irradiation time = 80 min

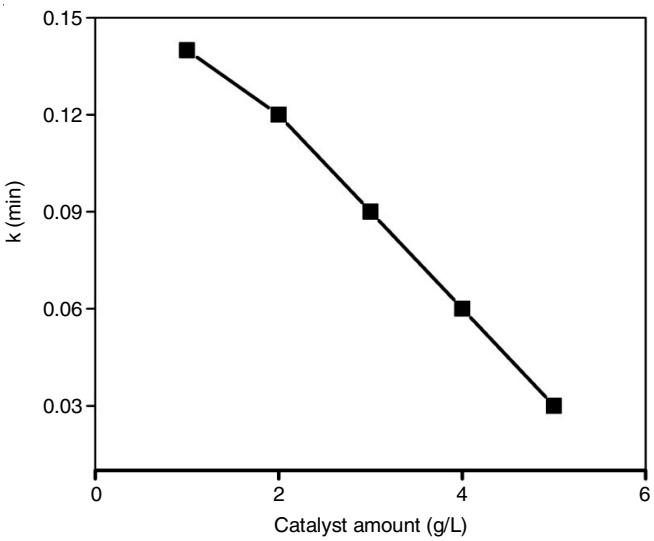


Fig. 10. Effect of catalyst loading, [methylene blue] =$10^{-5}$ mol $L^{-1}$, catalyst used = 8 wt % Eu–ZnO–Ag nanoparticles, pH = 11, irradiation time = 80 min

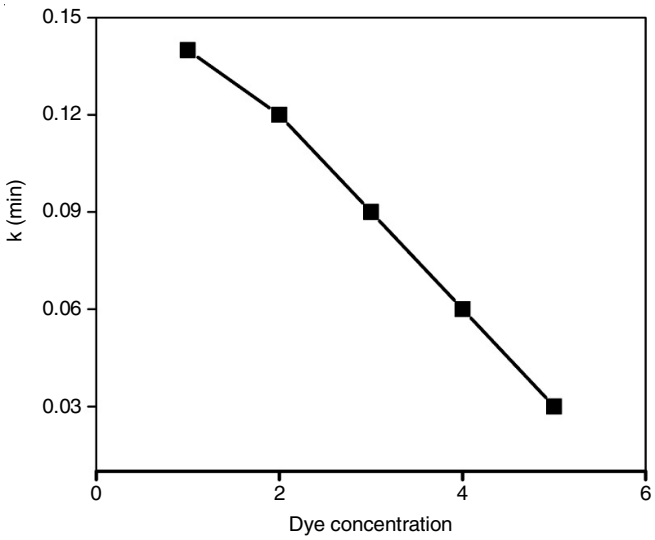


Fig. 11. Effect of initial concentration of methylene blue on irradiation with LED lights in the presence 8 % Eu–ZnO–Ag nanoparticles; pH = 11, catalyst suspension = 0.50 g $L^{-1}$ at different initial concentration

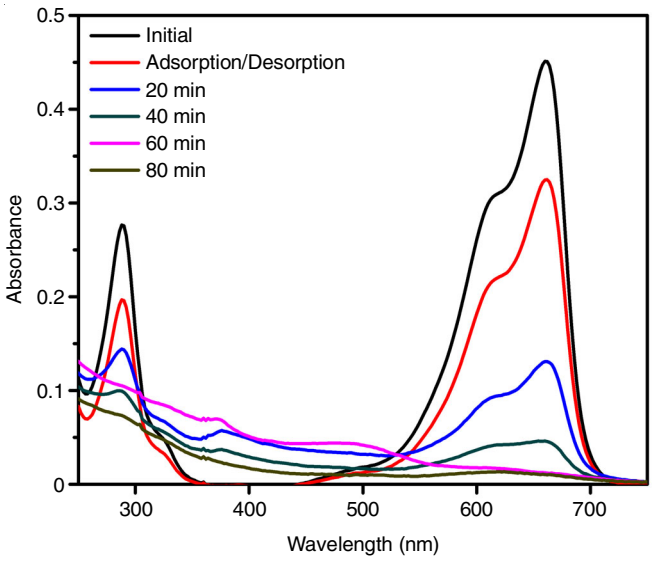


Fig. 12. UV-visible spectra on irradiation of methylene blue with LED light in the presence of 8 % Eu–ZnO–Ag: [methylene blue] = $10^{-5}$ M; pH = 11; catalyst suspension = 0.5 g $L^{-1}$; at different time intervals

$min^{-1}$) for nanoparticles. The degradation reaction rate decreases with increasing catalyst dosage amount. The Eu–ZnO-Ag nanoparticles surface area of catalyst may influence rate of the reactions. The rate of degradation decreased in methylene blue at higher dosage may be due to light absorption effect by the catalyst.

**Effect of initial dye concentration:** Fig. 11 showed a range of initial concentrations of methylene blue degradation on Eu–ZnO-Ag was investigated. Influence of dye concentration from 1-5 × $10^{-4}$ M photo-degradation from 0.1370 to 0.0262 $min^{-1}$ at 30 min the rate constant was decrease linearly. The photodegradation efficiency is low in higher concentration due to the light absorption by catalyst and dye molecules.

**Photodegradability of methylene blue with LEDs/Solar illuminations:** The photo-catalytic activity of methylene blue with Eu–ZnO-Ag and doped/undoped ZnO nanoparticles under LEDs illuminations in different time intervals (Fig. 12). Nearly complete degradation was observed in 80 min of methylene blue molecules with Eu–ZnO-Ag under LEDs light. Photo-degradation (0.4 %) slight occurred while the reaction was studied in presence of LEDs without any photo-catalyst, The same experiment performed on Eu–ZnO-Ag in absence of LEDs light we absorbed 24 % of dye molecule removed, which may be due to adsorption of the methylene blue by catalyst. From these annotations, We concluded that effective degradation of the methylene blue dye performed by the both LEDs and photocatalyst [18,22,23].

When the photocatalytic activity of Ag–ZnO, bare ZnO nanoparticles were used in same conditions 32 and 37 % degradations occurred, compared to others more efficient occurred in LEDs/Eu–ZnO-Ag nanoparticles degradation of methylene blue dye molecules (Fig. 13). The methylene blue degradation study containing Eu–ZnO-Ag obeys pseudo-first order kinetics. At low initial methylene blue dye concentration, the pseudo-first rate equation by:

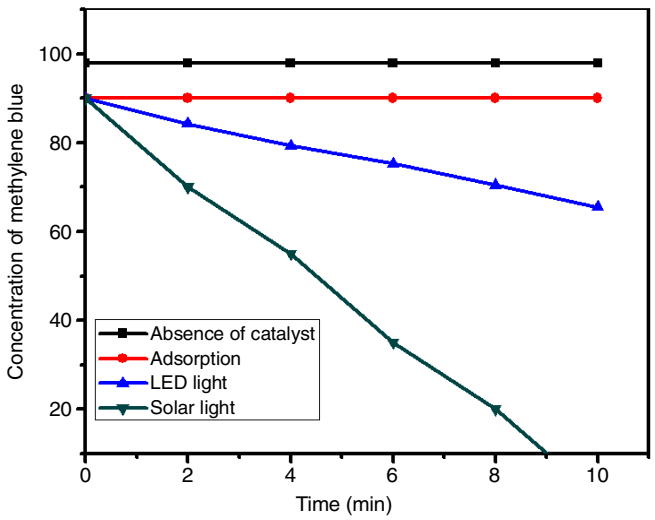


Fig. 13. Comparison of photodegradability of methylene blue between solar and LED lights; dye concentration = $10^{-5}$mol $L^{-1}$, catalyst suspension = 0.5 $g^{1}$, pH = 11 with %8 Eu–ZnO–Ag nanoparticles

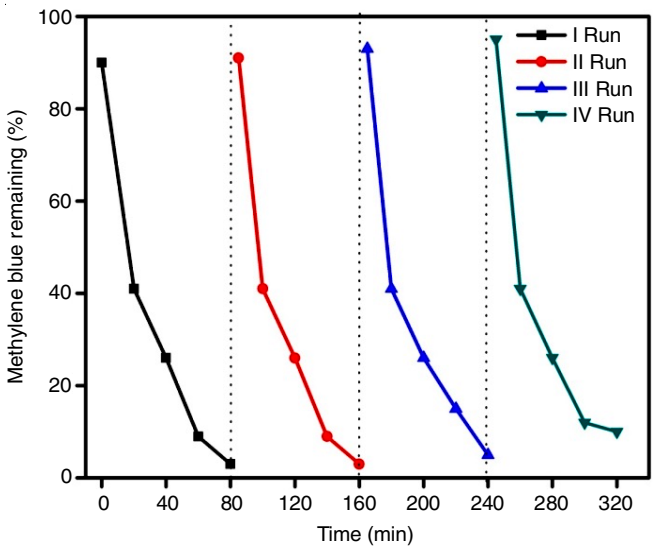


Fig. 14. Catalyst reusability, [methylene blue] dye concentration = $10^{-5}$ mol $L^{-1}$ catalyst suspension (8 % Eu–ZnO–Ag nanoparticles) = 0.5 g $L^{-1}$, pH = 11 LED and solar lights

$$d[C]/dt = k_0[C] \quad (1)$$

where $k_0$ is the pseudo-first order rate constant, C is methylene blue dye concentration. The surface photocatalyst on the adsorption–desorption equilibrium is reach methylene blue dye molecule at 30 min. After adsorption, the equilibrium dye solution with catalyst is resolute and is taken as the initial dye concentration for chemical kinetic degradation. Further modified of eqn. 2:

$$\ln(C_0/C) = k_0t \quad (2)$$

where $C_0$ is the equilibrium concentration of methylene blue dye and C is the concentration at time t. The absorption spectra of methylene blue dye ($5 \times 10^{-4}$ M) solution at different irradiation periods in Fig. 14. The UV-visible spectra in irradiation and the intensity at $\lambda_{max}$ 660 nm decreases regularly during the photo-degradation. This reveals that the intermediates $\lambda_{max}$ 380 nm peaks absorb after 20 min degradation due to some aromatic amine compounds present in solution. In presence of solar light 28 % methylene blue dye absorption/desorption occurred in the experiment perform with 8 % Eu–ZnO-Ag (without solar light). A very poor (3 %) degradation absorbed when the same experiment in methylene blue with solar light (without catalyst). More efficient phtodegradation of methylene blue dye depending on solar light and calalysts. The photocatalysts bare ZnO, Ag–ZnO, Eu–ZnO-Ag nanoparticles, were used under the same conditions, 60, 65.9, 85.3, 91.4, 100 % degradations occur (Fig. 15), respectively. The 8 % Eu–ZnO-Ag catalyst is excellent efficient than compared to related catalyst for photo-degradation of methylene blue (Fig. 15). It is clear that the solar degradation is much better than LED degradation.

**Stability and reusability of photo-catalyst:** The excellent performance of heterogeneous photo-catalysts used for many reactions is its reusability. The reusability of Eu–ZnO-Ag nanoparticles verified by four consecutive cycles for the photo-degradation of methylene blue dye (Fig. 14).

**Mechanism of degradation:** The photocatalyst study degradation of methylene blue dye illuminate by LEDs/solar

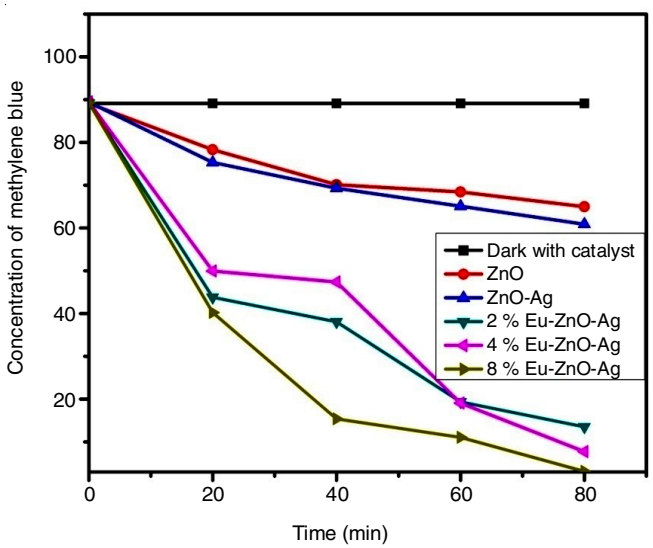


Fig. 15. Photodegradability of methylene blue; dye concentration = $10^{-5}$ mol $L^{-1}$, catalyst suspension = 0.5 g $L^{-1}$, pH = 11 with ZnO bare and Eu–ZnO–Ag nanoparticles

irradiation [22,23], a valence band electron goes to the conduction band leaving a hole in the valance band, regularly. These electron–hole pairs explain the activity of photocatalyst. Though, the presence of 'Eu' and 'Ag' traps the electron from the conduction band of ZnO concurrently, which suppress the electron–hole generated. It is well-known that 'Ag' can trap the electrons from the conduction band of ZnO during the presence of irradiation source in the photocatalytic degradation of methylene blue dye molecule. This excellent the photocatalytic behaviour of Eu–ZnO-Ag due to a electron-trapped between Ag and Eu in ZnO nanoparticles. Fig. 8 showed that the photocatalytic activity of Eu–ZnO-Ag nanoparticles is higher than that of pure and monodoped ZnO nanoparticles.

The mechanism of photocatalyst suggest itself electron trap from the photo-generated in oxygen adsorbed on the surface of photocatalyst and the electron shift to $O_2$ molecule its connecting catalyst on rate-determining step. on the other hand, $Eu^{3+}$

easily traps the photo-excited electronin the system of Eu-doped catalyst, because $Eu^{2+}$ ion, act as Lewis acid, it appears that is superior to the oxygen molecule ($O_2$) in its ability of trapping electrons [13,14,18]. The electrons trapped in $Eu^{2+}$ sites are consequently transferred due to the $O_2$ adsorbed by an oxidation process, so the band gap and holes is reduced (**Scheme-II**).

$$*Dye + Eu–ZnO–Ag \longrightarrow Dye + Eu–ZnO–Ag + e_{cb^-}$$

$$e_{cb^-} + O_2 \longrightarrow O_2^{\bullet-}$$

$$Dye^{\bullet-} + O_2/O_2^{-} \longrightarrow \text{Degradation products}$$

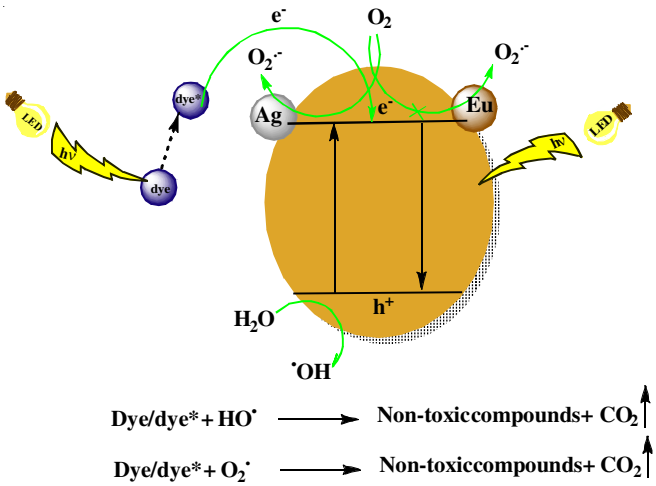


**Scheme-II:** Enhanced photocatalytic activity mechanism of Eu–ZnO–Ag nanoparticles in present of LED/solar lights illuminations

The activity of Eu 4*f* level in Eu–ZnO-Ag acting an important role in the interfacial electron transfer and electron–hole inhibition generation. The optical spectra showed that doping of Ag and Eu excellent the visible light absorption of catalyst and engender more electron–hole pairs in LEDs/solar light illumination, which enhanced to increase the photocatalytic activity of Eu–ZnO-Ag nanoparticles. Since $Eu^{2+}$ traps the electron straight forwardly, its act as a scavenger of electrons. So $Eu^{2+}$ and $Eu^{3+}$ accessible in Eu–ZnO-Ag influence the photoreactivity by shifting the electron–hole pair formed. Moreover, the trapping nature of Ag and $Eu^{2+}/Eu^{3+}$ sites are consequently transferred to the adjacent adsorbed $O_2$ to produce a great number of superoxide radical anions. The well reactive hydroxyl radicals and superoxide radical anion show the way to the methylene blue dye degradation. The excellent creation of $O_2^{\bullet-}$ and $^{-}OH$ by Eu and Ag increases the photocatalytic activity of Eu-ZnO-Ag nanoparticles.

## Conclusion

The successfully synthesized (Eu-ZnO-Ag) nanoparticles by precipitation-decomposition method. The characterization of photo-catalyst by XRD, FE-SEM images, EDS, optical measurements. The absorption of ZnO to doped ZnO nanoparticles are swing visible region due to dopants (Ag/Eu). Eu-ZnO-Ag photocatalyst shows lower reflectance (high absorption) in the visible region than pure ZnO and shifting of the absorption edge to moved visible region. The photoluminescence spectra explained the self-consciousness of photo electron–hole pairs by loading dopants (Eu/Ag) on ZnO nanoparticles. The dopants are $Eu^{2+}$ and 'Ag' trap the photo-excited electrons in solution, so decreasing rate of the electron–hole pairs in catalyst. Excellent photodegradation efficient Eu-ZnO-Ag nanoparticles comparted to commercial ZnO, bare ZnO, Eu–ZnO, Ag–ZnO. The optimum catalyst dosage and pH of solution for completely removal of methylene blue dye. A mechanism of excellent photocatalytic activity of Eu-ZnO-Ag nanoparticles showed electron trapping by dopants. The Eu-ZnO-Ag nanoparticles playing reusable photocatalyst.

## CONFLICT OF INTEREST

The authors declare that there is no conflict of interests regarding the publication of this article.

## REFERENCES


1. U.I. Gaya and A.H. Abdullah, *J. Photochem. Photobiol. Photochem. Rev.*, **9**, 1 (2008); https://doi.org/10.1016/j.jphotochemrev.2007.12.003.
2. K. Nakata and A. Fujishima, *J. Photochem. Photobiol. Photochem. Rev.*, **13**, 169 (2012); https://doi.org/10.1016/j.jphotochemrev.2012.06.001.
3. A. Fujishima and K. Honda, *Nature*, **238**, 37 (1972); https://doi.org/10.1038/238037a0.
4. I. Muthuvel and M. Swaminathan, *Catal. Commun.*, **8**, 981 (2007); https://doi.org/10.1016/j.catcom.2006.10.015.
5. I. Muthuvel, B. Krishnakumar and M. Swaminathan, *J. Environ. Sci.*, **24**, 529 (2012); https://doi.org/10.1016/S1001-0742(11)60754-7.
6. H. Huang, D.Y.C. Leung, P.C.W. Kwong, J. Xiong and L. Zhang, *Catal. Today*, **201**, 189 (2013); https://doi.org/10.1016/j.cattod.2012.06.022.
7. M. Lazar, S. Varghese and S. Nair, *Catalysts*, **2**, 572 (2012); https://doi.org/10.3390/catal2040572.
8. M.V. Enoch, R. Rajamohan and M. Swaminathan, *Spectrochim. Acta A Mol. Biomol. Spectrosc.*, **77**, 473 (2010); https://doi.org/10.1016/j.saa.2010.06.021.
9. S. Singhal, J. Kaur, T. Namgyal and R. Sharma, *Physica B*, **407**, 1223 (2012); https://doi.org/10.1016/j.physb.2012.01.103.
10. R. Chauhan, A. Kumar and R.P. Chaudhary, *J. Sol-Gel Sci. Technol.*, **63**, 546 (2012); https://doi.org/10.1007/s10971-012-2818-3.
11. D. Daniel and I.G.R. Gutz, *Electrochem. Commun.*, **9**, 522 (2007); https://doi.org/10.1016/j.elecom.2006.10.014.
12. S. Han, Y. Tang, H. Guo, S. Qin and J. Wu, *Nanoscale Res. Lett.*, **11**, 273 (2016); https://doi.org/10.1186/s11671-016-1497-3.
13. A.R. Khataee, A. Karimi, R.D.C. Soltani, M. Safarpour, Y. Hanifehpour and S.W. Joo, *Appl. Catal. A Gen.*, **488**, 160 (2014); https://doi.org/10.1016/j.apcata.2014.09.039.
14. A. Phuruangrat, O. Yayapao, T. Thongtem and S. Thongtem, *J. Nanomater.*, **2014**, Article ID 367529 (2014); https://doi.org/10.1155/2014/367529.
15. S. Anandan, Y. Ikuma and V. Murugesan, *Int. J. Photoenergy*, **2012**, Article ID 921412 (2012); https://doi.org/10.1155/2012/921412.
16. R. Kumar, A. Umar, G. Kumar, M.S. Akhtar, Y. Wang and S.H. Kim, *Ceram. Int.*, **41**, 7773 (2015); https://doi.org/10.1016/j.ceramint.2015.02.110.
17. C. Jayachandraiah, K.S. Kumar, G. Krishnaiah and N.M. Rao, *J. Alloys Compd.*, **623**, 248 (2015); https://doi.org/10.1016/j.jallcom.2014.10.067.
18. Y.J. Jose, M. Manjunathan and S.J. Selvaraj, *J. Nanostruct. Chem.*, **7**, 259 (2017); https://doi.org/10.1007/s40097-017-0236-3.
19. N. Rajendiran and M. Swaminathan, *Spectrochim. Acta A Mol. Biomol. Spectrosc.*, **52**, 1785 (1996); https://doi.org/10.1016/S0584-8539(96)01704-7.
20. N.V. Kaneva, D.T. Dimitrov and C.D. Dushkin, *Appl. Surf. Sci.*, **257**, 8113 (2011); https://doi.org/10.1016/j.apsusc.2011.04.119.
21. S. Velanganni, S. Pravinraj, P. Immanuel and R. Thiruneelakandan, *Physica B*, **534**, 56 (2018); https://doi.org/10.1016/j.physb.2018.01.027.
22. B. Subash, B. Krishnakumar, R. Velmurugan, M. Swaminathan and M. Shanthi, *Catal. Sci. Technol.*, **2**, 2319 (2012); https://doi.org/10.1039/c2cy20254a.
23. W.-K. Jo and R.J. Tayade, *Chin. J. Catal.*, **35**, 1781 (2014); https://doi.org/10.1016/S1872-2067(14)60205-9.